Acta Chemica Scandinavica A 38 (1984) 563–573

Magnetic and Structural Properties of Transition Metal Substituted MnP. I. $Mn_{1-t}Co_tP$ ($0.00 \leq t \leq 0.30$)

HELMER FJELLVÅG and ARNE KJEKSHUS

Kjemisk Institutt, Universitetet i Oslo, Blindern, Oslo 3, Norway

$Mn_{1-t}Co_tP$ is studied for $0.00 \leq t \leq 0.30$ by X-ray and neutron diffraction at and below room temperature and applied magnetic fields up to 15.6 kOe. The MnP type atomic arrangement prevails under these conditions, in para-, ferro- or various (essentially) helimagnetic states. The magnetic characteristics of $Mn_{1-t}Co_tP$ are compared and discussed in terms of the available information on MnP.

Manganese monophosphide, the prototype of the MnP type structure, is an interesting compound which has attracted considerable attention over the years. Although almost all conceivable properties, effects and/or methods have been examined on/for MnP (*cf.*, *e.g.*, Ref. 1), it is certainly its rather unique magnetic features which have kept the substance popular for a long time.

In a series of papers we will report on structural and magnetic properties of transition metal substituted MnP, *viz.* $Mn_{1-t}T_tP$ with T=V, Cr, Fe, Co, Ni, Mo and W. Some of the magnetic characteristics for T=V, Cr, Fe and Co are also dealt with in an earlier communication.[2] The present report concerns $Mn_{1-t}Co_tP$, but since the results are derived from powder samples, a comparison with, and a brief survey of, the situation for MnP itself is pertinent.

EXPERIMENTAL

Samples were made from 99.99 % Mn, 99.999 % Co (Johnson, Matthey & Co. crushed Mn flakes, turnings from rods of Co) and 99.999 % P (Koch-Light Laboratories; lumps of red P). MnP and CoP were synthesized by heating stoichiometric quantities of the elements in evacuated, sealed quartz tubes. The preparational procedure for CoP followed the description in Ref. 3, whereas that for MnP differed somewhat. Double quartz tubes were always used for MnP. These were placed in the horizontally positioned furnaces and the temperature was slowly increased (3×30 °C per day) to 900 °C, kept there for 2 d and cooled to room temperature over 1 d. The samples were then crushed and subjected to one further heat treatment at 900 °C for 3 d, followed by cooling to room temperature over 1 d. Ternary $Mn_{1-t}Co_tP$ samples were made from the binary compounds. After a first heat treatment at 1000 °C for 1 week, the samples were crushed and reheated at 950 °C for 1 week, and finally cooled to room temperature over 1 d. The homogeneity, composition and structural state of the samples were ascertained from powder X-ray (Guinier) diffraction photographs.

Experimental details concerning the X-ray and neutron diffraction measurements are described in Refs. 4, 5. The nuclear neutron scattering lengths (in 10^{-12} cm) $b_{Mn}=-0.37$, $b_{Co}=0.28$ and $b_P=0.51$ were taken from Ref. 6, and the magnetic form factor for Mn^{2+} from Ref. 7.

RESULTS AND DISCUSSION

(i) *Atomic arrangement.* In accordance with Ref. 3, $Mn_{1-t}Co_tP$ with $0.00 \leq t \leq 0.30$ takes the MnP type atomic arrangement at, and below, room temperature. (The present description of the MnP type structure is based on *Pnma*, $c>a>b$, setting of the unit cell.) The Bragg reflections are generally sharp and no additional

0302-4377/84 $2.50

Table 1. Unit cell dimensions and positional parameters with standard deviations for $Mn_{1-t}Co_tP$ as derived by Rietveld analysis of powder neutron diffraction data. Space group *Pnma*; Mn/Co in 4*c* and P in 4*c*. (Nuclear R_n-factors ranging between 0.03 and 0.05; magnetic R_m-factors ranging between 0.05 and 0.08; profile R_p-factors ranging between 0.08 and 0.11.)

t	T (K)	*a* (pm)	*b* (pm)	*c* (pm)	x_T	z_T	x_P	z_P
0.00	293	526.01(4)	317.41(2)	591.93(4)	0.0061(11)	0.1962(12)	0.1884(8)	0.5690(7)
	60	524.09(3)	318.06(2)	590.27(4)	0.0074(11)	0.1962(9)	0.1881(8)	0.5700(6)
	10	524.16(4)	318.02(2)	590.32(5)	0.0056(14)	0.1952(12)	0.1879(9)	0.5696(8)
0.05	293	524.85(9)	316.77(5)	590.38(2)	0.0070(10)	0.2002(10)	0.1868(6)	0.5698(7)
	60	523.65(3)	317.90(2)	589.52(4)	0.0057(11)	0.1972(10)	0.1875(7)	0.5696(8)
	10	523.65(4)	317.81(2)	589.46(4)	0.0069(11)	0.1989(11)	0.1862(7)	0.5705(8)
0.10	293	524.63(5)	316.70(3)	590.10(6)	0.0073(17)	0.1975(18)	0.1910(9)	0.5691(8)
	60	523.09(5)	317.69(3)	588.70(5)	0.0067(16)	0.1969(13)	0.1874(9)	0.5716(8)
	10	523.06(5)	317.70(3)	588.62(6)	0.0051(16)	0.1992(17)	0.1878(9)	0.5705(7)
0.20	293	522.96(7)	316.83(4)	587.75(8)	0.0061(21)	0.1940(20)	0.1903(10)	0.5699(9)
	85	521.45(7)	317.03(4)	586.30(8)	0.0071(29)	0.1950(20)	0.1900(14)	0.5723(11)
	10	521.29(8)	317.19(4)	586.01(9)	0.0085(25)	0.1960(23)	0.1910(14)	0.5720(10)
0.30	293	520.57(7)	317.20(4)	584.12(8)	0.0023(20)	0.1925(22)	0.1938(19)	0.5701(17)
	10	519.27(7)	316.76(3)	582.95(7)	0.0031(24)	0.1929(21)	0.1944(17)	0.5714(16)

superstructure reflections are observed in the X-ray and neutron diffraction diagrams. Hence, the random, long range distribution of Mn and Co over the metal sub-lattice should be substantiated. The unit cell dimensions and positional parameters (as derived from powder neutron diffraction data) are listed in Table 1.

As seen from Table 1 the positional parameters remain unchanged within two calculated standard deviations upon variation of composition ($0.00 \leq t \leq 0.30$) and temperature ($10 \leq T \leq 293$ K). The constancies and the numerical values of the positional parameters are consistent with the geometrical considerations in Refs. 8, 9 as well as the fact[3] that $Mn_{1-t}Co_tP$ crystallizes with the MnP type structure from 10 to (at least) 1400 K. The increase in the calculated standard deviations of x_T and z_T with increasing *t* is mainly due to the corresponding reduction in the effective scattering length of *T*.

The variations of the unit cell dimensions of $Mn_{1-t}Co_tP$ with *t* at 10 and 293 K are illustrated in Fig. 1. The data shown for 293 K are entirely consistent with those published by Selte *et al.*,[3] the minimum in *b versus t* being partly blurred by the narrower scale used in Ref. 3. The temperature behaviour of the *b* axis appears to be a sensitive indicator of ferro (F) and/or helimagnetic (H_c) states.[4,5] The observation that *b* is expanded between 293 and 10 K for $0.00 \leq t < \sim 0.25$ (Fig. 1) therefore suggests that the F and/or H_c phases prevail over the said compositional range [see (ii) and Ref. 2].

Powder neutron diffraction data have also been recorded under different externally applied magnetic fields ($0.0 \leq H \leq 15.6$ kOe; at temperatures between 22 and 80 K). Although the aim of this part of the study has been to elucidate the magnetic properties of $Mn_{1-t}Co_tP$, contours of the response of the crystal structure on an external field have come to hand. Due to the long neutron wavelength ($\lambda \approx 405$ pm) used to explore details of the magnetic $000^{\pm}$ satellite the only accessible nuclear reflections were 101, 011 and 002. The thus limited data suggest that the positional parameters are essentially unaffected by the external magnetic fields used in this study. Nor do the unit cell dimensions experience marked changes under the influence of the external magnetic fields. The *c* axis appears to increase with increasing external field and this behaviour is more pronounced in the H_c than the $H_{c,fan}$ phase [see (iii)].

(ii) *Magnetic structures and their variations with composition and temperature.* The magnetic phase diagram for $Mn_{1-t}Co_tP$[2] for $0.00 \leq t \leq 0.30$ and $0 < T < 300$ K comprises the stability ranges of the P (paramagnetic), F and H_c phases. The

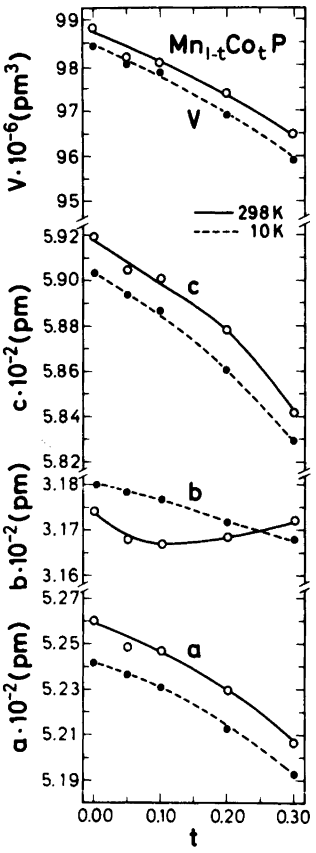

Fig. 1. Unit cell dimensions of $Mn_{1-t}Co_tP$ *versus* t ($0.00 \leq t \leq 0.30$) at 10 and 293 K. *Calculated* error limits do not exceed size of symbols. (1 Å=10^2 pm.)

consistency with this work is ensured by the fact that the present data were taken into account when the diagram in Ref. 2 was constructed.

The extension of the F phase is confirmed up to t=0.20 by the neutron diffraction technique, and including also the magnetization data[2] the F phase limit occurs at $0.25<t<0.30$. No indication of any cooperative phenomenon could be detected by careful examination of the various neutron diffraction diagrams of $Mn_{0.70}Co_{0.30}P$ ($10 \leq T \leq 293$ K). The Curie temperature (T_C for the F⇄P transition) decreases with t, values of 292±4, 275±5, 225±5 and 150±10 K being found by neutron diffraction for t=0.00, 0.05, 0.10 and 0.20, respectively. T_C=292±4 K obtained for MnP itself is in full accordance with the values given in the literature (*cf.* Ref. 1 which lists recent T_C values between 290 and 291.5 K as determined by several research groups, various methods and differently prepared samples).

The magnetic moment (μ_F) of the F phase is found to be arranged parallel to the crystallographic b axis for $Mn_{1-t}Co_tP$ with $0.00 \leq t \leq 0.20$ (*cf.* Ref. 2), and μ_F decreases with increasing t. Numerical data for t, μ_F (in μ_B) are: 0.00, 1.43(4) at 60 K; 0.05, 1.37(5) at 60 K; 0.10, 1.25(5) at 60 K; 0.20, 0.81(5) at 85 K, with calculated standard deviations given in the parentheses. The present data for the magnetic structure of the F phase of MnP are compatible with earlier findings (*cf.* Ref. 1 and references therein).

At T_S the F phase transforms into the H_c phase for $Mn_{1-t}Co_tP$ with $0.00 \leq t \leq 0.20$. The numerical values for T_S in Table 2 show that this parameter stays virtually constant between t=0.00 and 0.10 whereupon a fairly rapid increase in T_S follows. As opposed to the second order F⇄P transformation, the H_c to F transition in MnP is reported to be of first order (*cf.* Ref. 1). The hysteresis which accompany the H_c to F transition in MnP is extremely narrow (~0.25 K hysteresis compared with an overall width of ~0.5 K for the transition according to Ref. 10) and is difficult to detect even for single crystal samples (*cf.* Refs. 10 and 11). The situation is more complex and unclear for powder samples, where the H_c to F or *vice versa* transition, as *e.g.* demonstrated by the temperature variation of the integrated intensity of the $000^{\pm}$ satellite, is rather

Table 2. Helimagnetic parameters for $Mn_{1-t}Co_tP$ at 10 K.

t	$\tau_c/2\pi c^*$	μ_H (μ_B)	$\phi_{1,2}$ (°)	T_S (K)
0.00	0.116±0.002	1.45±0.04	24±3	53±3
0.05	0.102±0.002	1.40±0.05	15±3	49±3
0.10	0.109±0.002	1.21±0.04	19±3	47±3
0.20	0.112±0.002	1.02±0.05	20±3	75±2

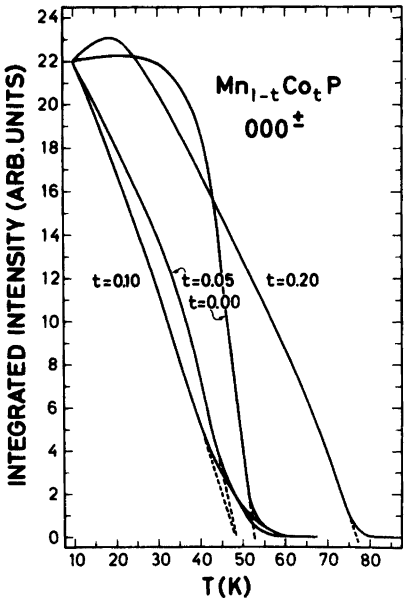

Fig. 2. Integrated intensity of $000^{\pm}$ *versus* temperature for $Mn_{1-t}Co_tP$ with t=0.00, 0.05, 0.10 and 0.20.

broad (see Fig. 2 and *vide infra*). However, despite several attempts a hysteresis feature of the H_c to F transition for $Mn_{1-t}Co_tP$ with $0.00 \leq t \leq 0.20$ could not be substantiated in this study.

The present value of T_S=53±3 K for MnP concurs with the recent results of Takase and Kasuya.[12] According to the latter authors, T_S (as opposed to T_C) is very sensitive to the purity of the samples, and in this way they explain the scattered T_S values (47 to 53 K) found in the literature (*cf.* Ref. 1 and references therein). However, the kind of impurity is certainly not immaterial in this context. In fact, none of the $Mn_{1-t}T_tP$ and $MnP_{1-x}X_x$ solid solution phases which we have examined appears to provide impurity candidates for the relatively large variation of T_S. Takase and Kasuya[12] use the residual resistivity ratio, rather than analytical data, as an indicator of sample purity/impurity. Since they (and other authors) moreover studied samples prepared from the melt, some (difficult controlled) variation in the Mn:P atomic ratio (*viz.* deviation from the stoichiometric 1:1 composition) may perhaps be expected. Crystalline imperfections in the form of vacancies and/or

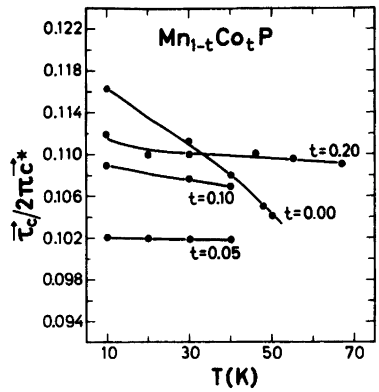

Fig. 3. Temperature dependences of the propagation vector (τ_c) for $Mn_{1-t}Co_tP$ with t=0.00, 0.05, 0.10 and 0.20.

interstitials are known (from other cases) to have a pronounced effect on the residual resistivity ratio, and a corresponding influence on T_S seems very likely. However, further data are required to resolve this problem.

Since the present study has been confined to powder samples, the original and simplest model[11,13] for the magnetic structure of the H_c phase of MnP was adopted for $Mn_{1-t}Co_tP$. The model and some experimental facts are summarized in Ref. 4. Numerical values for the variable parameters of this model (*viz.* the propagation vector τ_c of the spirals, the helimagnetic moment μ_H and the phase angle $\phi_{1,2}$ between the spirals through atoms 1 and 2) are given in Table 2 for $Mn_{1-t}Co_tP$.

The data for MnP in Table 2 concur reasonably well with those found in the literature[11,13,14] when the simplifying features of the present model are taken into account. For τ_c, which is easy to determine accurately because it concerns only the position of the satellites, there is almost perfect match between the various studies, and $\tau_c/2\pi c^*$=0.117±0.002[14] represents the most probable value for MnP at 4.2 K. (As seen from the temperature dependence for t=0.00 in Fig. 3, τ_c for MnP should be referred to a particular temperature.)

The present values for μ_H and $\phi_{1,2}$ are subject to larger uncertainties. Due to the few and weak satellites which are experimentally accessible by the powder neutron diffraction method, there occur systematic as well as random errors which affect the results. Clearly, also the choice of

magnetic form factor is of importance for estimation of μ_H and $\phi_{1,2}$ (more for the former than the latter). The influence of the form factor appears to provide a reasonable explanation of the large scatter between the earlier values[11,13,14] μ_H=1.3±0.1, 1.57 (average) and 1.25 μ_B (average), which are all based on single crystal data. μ_H=1.33 μ_B (as also obtained by magnetization measurements[2,14]) is a probable value for MnP and is consistent with no change in magnetic moment at the F to H_c transition. The present value of μ_H=1.45±0.04 μ_B for MnP is on this background a little too high (and the estimated errorlimit which neglects the systematic errors is certainly too optimistic). However, the compositional variation of μ_H for $Mn_{1-t}Co_tP$ is believed to be correctly brought out in Table 2.

The earlier findings for $\phi_{1,2}$ (of 16 and 16.1±0.2° in Refs. 11 and 13; $\phi_{1,2}$ is not reported in Ref. 14) are in excellent agreement. $\phi_{1,2}$=24±3° found in this study is again a little too high, but this discrepancy should not be stressed in view of the possible systematic errors in the present sparse data. The attention should rather be focused on the approximate compositional (t) independence (within the expectedly correct relative errorlimits) of $\phi_{1,2}$ (Table 2).

Due to the fact that reasonably accurate intensity assessments for satellites other than $000^{\pm}$ are difficult to obtain for the present samples, less decisive information on the temperature variation of μ_H and $\phi_{1,2}$ were obtained. The situation is, in part, reflected in the temperature variations of the intensity of $000^{\pm}$ for $Mn_{1-t}Co_tP$ (Fig. 2).

The combination of available data on $Mn_{1-t}T_tP$ phases (*cf.*, *e.g.*, Refs. 1, 3, 5, 14, 15) suggests very strongly that μ_H is virtually temperature independent for a given t. For $\phi_{1,2}$ there is no decisive evidence at all, but we *believe* that as a zeroth approximation also this parameter may be regarded as temperature independent.

In this situation it is appropriate to ask for an explanation of the gradual temperature variations of the intensity of $000^{\pm}$ in Fig. 2 as opposed to the (approximate) step-wise behaviour expected for an idealized case where μ_H and $\phi_{1,2}$ stay constant over the stability range of the H_c mode. In order to penetrate a little into this problem, the intensity variation in $000^{\pm}$ with $\phi_{1,2}$ as the single variable (*viz.* all crystallographic parameters, τ_c and μ_H are kept constant) were calculated. As seen from Fig. 4, the normalized intensity of $000^{\pm}$ shows a periodic dependence on $\phi_{1,2}$ under such conditions. [The functional relationship for $000^{\pm}$ is identical for the H_c and H_a modes (*cf.*, *e.g.*, Ref. 4).] A corresponding functional relationship exists for all satellites of

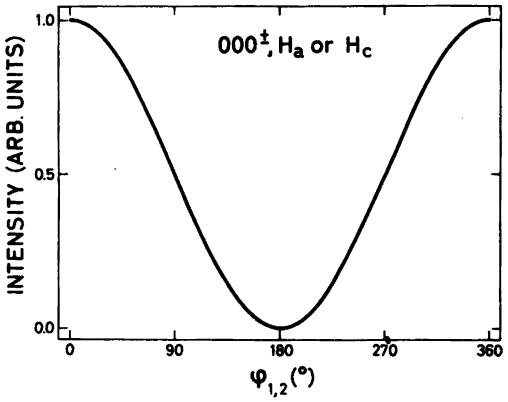

Fig. 4. Model calculations of intensity *versus* $\phi_{1,2}$ for $000^{\pm}$. Maximum at 0°. For constraints of the computational model see text.

the H_c (and H_a) modes under the above specified conditions. The individual distinction of the various satellites is a shift of the curve along the $\phi_{1,2}$ axis of Fig. 4. For, say, 101^- and 101^+ of the H_c mode the maxima are shifted to 140 and 220°, respectively. For all satellites the maximum and minimum in $\phi_{1,2}$ are separated by 180°.

Comparison of Figs. 2 and 4 reveals some resemblance in curve shape. However, it seems physically unmotivated to suggest that a substantial variation of $\phi_{1,2}$ over, say, 150° should account for the observed temperature dependences of the integrated intensity of $000^{\pm}$ in Fig. 2. Compositional variation within the samples can similarly be ruled out as a cause of the unsharp H_c to F transitions. Neither the nuclear nor the satellite reflections for $Mn_{1-t}Co_tP$ are broader than expected. Hence, it seems that the explanation must be sought in thermally induced disorder and/or imperfections of the magnetic spiral structure. However, the sparse experimental data and the many possibilities for disordering of the quite complex MnP,H_c type magnetic structure makes it pointless to pursue the problem further.

It should be mentioned that the present model for the MnP,H_c type magnetic structure represents a good approximation of the more refined models considered in Refs. 13, 14, 16. According to these models there occur deformations of the spirals. Forsyth *et al.*[13] introduced the concept of elliptical spirals and concluded that the components of the moments along the *a* and *b* axes are, respectively, 1.41±0.10 and 1.73±0.10 μ_B (*viz.* a moment ratio of 1.23±0.16). The bunching model where the moments are allowed to be more crowded in certain directions within the *ab* planes

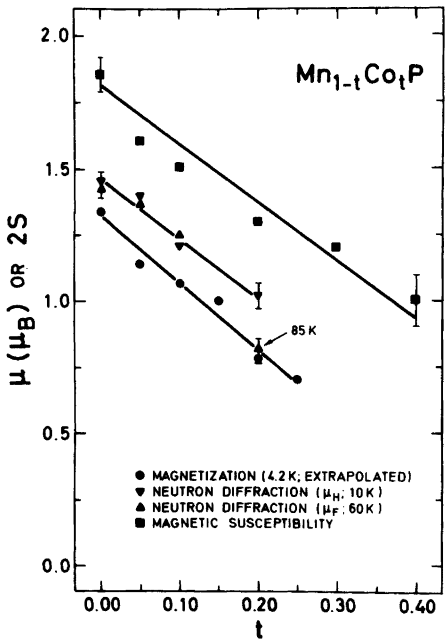

Fig. 5. Extrapolated magnetization moments (taken from Ref. 3), neutron diffraction μ_F and μ_H moments and paramagnetic $2S$ values ("spin only" approximation; taken from Ref. 2) *versus* the compositional parameter t. Legends to symbols are given on the illustration. Bars represent estimated or calculated errors.

are proposed on theoretical basis by Hiyamizu and Nagamiya.[17] Using the bunching model Obara *et al.*[14] arrived at moments of 1.20±0.05 and 1.29±0.10 μ_B along the *a* and *b* axes, respectively (*viz.* a moment ratio of 1.08±0.13), and concluded that there was no significant distortion from circularity of the spirals. However, Moon[16] recently reported that the bunching model applies to MnP (with moment ratio 1.091±0.007) and presented third order satellites as evidence for this view. The question of whether or not the spirals are deformed is therefore apparently settled. The mutual discrepancies between the three[13,14,16] well conducted single crystal studies clearly indicate that data of high quality (better than the present powder data) are needed to attack problems of this complexity.

The relation between $2S$ (number of unpaired spins in paramagnetic state according to the "spin only" approximation; Ref. 3) and the magnetic moments deduced by neutron diffraction and magnetization (Ref. 2) measurements is depicted in Fig. 5. The results obtained by the three techniques display essentially three parallel lines which decrease with increasing t. (Note, however, that the $2S$ points are better approximated by a non-linear curve.) The findings in Fig. 5 will be discussed in relation to the corresponding data for all $Mn_{1-t}T_tP$ phases.

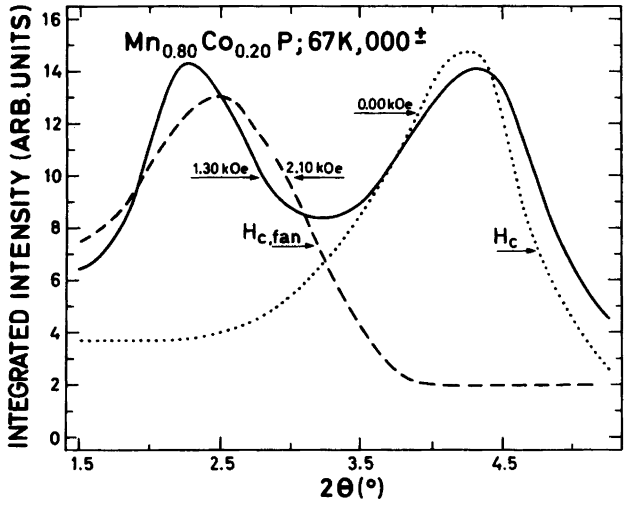

Fig. 6. Observed peak profile of 000± for $Mn_{0.80}Co_{0.20}P$ at 67 K and external fields of 0.00, 1.30 and 2.10 kOe. Experimental points are omitted for clarity. H_c denotes the *c* axis helical state and $H_{c,fan}$ the corresponding fan state.

(iii) *On influence of external magnetic fields on the helimagnetic structure.* Application of external magnetic fields may induce changes in the arrangements of the moments of the H_c and F phases of MnP,[14,18,19] and the recent results[14] suggest that the size of the moments is essentially independent of the external field. The situation is also retained in the pseudo-binary $Mn_{1-t}Co_tP$ phase, but since the present study has been limited to powder samples, mostly qualitative surveying information has been gathered. The fact that an external field modifies the (zero field) magnetic structure of the H_c phase is easily demonstrated by mapping the variation of the $000^{\pm}$ satellite with the applied field. The three experimental $000^{\pm}$ profiles for $Mn_{0.80}Co_{0.20}P$ at 67 K (Fig. 6) can serve as an example of the results thus obtained. The single $000^{\pm}$ characteristic of the H_c mode in zero field has developed into a doublet at 1.30 kOe. At 2.10 kOe the original peak has completely disappeared. Analogous observations have been recorded for MnP itself, the main distinctions being that the position of the peaks and the field dependences of their (relative and absolute) intensities are changed.

Fig. 6 and other results of this study can be rationalized on the basis of the current *H*,T phase diagram data for MnP. The *H*,T phase diagram for the magnetic structures in anisotropic substances like MnP vary according to the crystallographic orientation. The diagrams for **H** parallel to **a**[10,20,21] (intermediate axis) and **c**[22] (hard axis) are shown in Fig. 7. In addition to the zero field P (the symbol also referring to the spin aligned state), F and H_c phases, these diagrams also contain phases (magnetic structures) designated $H_{c,fan}$ and $H_{c,cone}$. Both these field induced magnetic states represent perturbations of a basic H_c arrangement of the moments. The $H_{c,fan}$ structure[18] differs from the H_c type in that the moments do not undergo a full rotation in the (001) plane, but rather oscillate about (or phrased differently are crowded near) the *b* direction. It is likely that $H_{c,fan}$ (marked with ?) of the lower diagram of Fig. 7 corresponds to that of the upper diagram. No neutron diffraction study has so far been reported for the magnetic structure designated $H_{c,cone}$ in Fig. 7, but this structure possibly consists of a ferromagnetic component along the spiral propagation direction (*c*) superimposed on the H_c arrangement. The

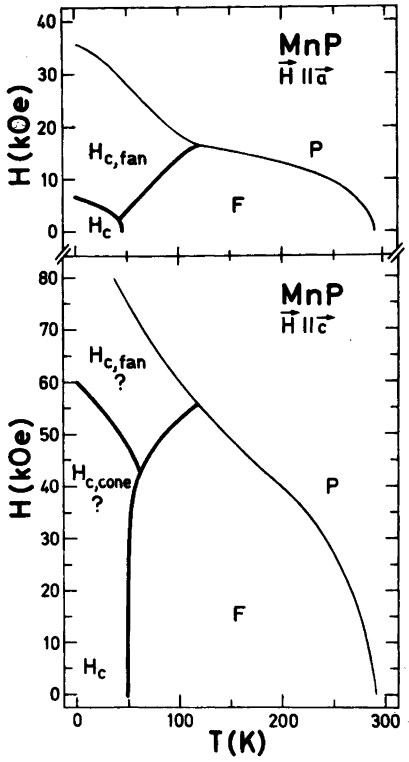

Fig. 7. *H*,T phase diagrams for MnP with **H**||**a** (upper) and **H**||**c** (lower). The diagrams are quoted from Refs. 10, 20. Magnetic state and/or structure is indicated by P para, F ferro, H_c *c* axis helical, $H_{c,fan}$ fan and $H_{c,cone}$ cone.

ratio of the moment components parallel and perpendicular to *c* defines the cone angle, which in turn depends on the magnitude of the applied field.

Thick and thin curves have been used to distinguish between, respectively, first and second (or higher) order phase transitions in Fig. 7. The P, F, $H_{c,fan}$ triple point in the upper diagram is a Lifshitz point,[10,19] whereas the F, H_c and $H_{c,fan}$ phases meet in a normal triple point. It has been suggested[23] that the two triple points in the lower diagram of Fig. 7 have corresponding characteristics to those in the upper diagram.

The additional *H*,T diagram (not shown in Fig. 6) for **H** parallel to **b** (easy axis) is the simplest of the three unique such diagrams. A first order H_c to F phase boundary which extends approximately linearly from $T = T_S$, $H = 0$ kOe to $T = 0$ K, $H \approx 2.5$ kOe and an isolated critical point at T

$= T_C$, $H = 0$ kOe are the prominent features of this diagram.[24]

Only single crystals exhibit clear-cut H,T diagrams of the type shown in Fig. 7. A powder sample of MnP with random orientation of the individual crystallites should show an H,T diagram which results from a superposition of the diagrams for the crystallographic axes. The averaging over the three unique (axial) H,T diagrams is complex, and the unavoidable degree of preferred orientation of the powder sample (in the magnetic field) makes it purposeless to put any effort into construction of a quantitative "powder H,T phase diagram" for MnP. However, an important qualitative feature of such a "powder H,T diagram" is broad transition regions and coexistence of two or more magnetic phases over considerable ranges of external fields. This is brought out in the present experimental data.

The two peaks in Fig. 6 can, on this background, be interpreted as arising from the phases H_c (possibly with an additional contribution from $H_{c,cone}$ in none zero fields) and $H_{c,fan}$. Their intensity variations with the applied field for MnP are shown in Fig. 8. The range of coexistence for $H_c/H_{c,cone}$ and $H_{c,fan}$ extends from ~4 to ~8 kOe. The maximum in the curve for $H_{c,fan}$ at ~8 kOe may reflect that the fan oscillations (*vide supra*) become more restricted at higher fields or that the orientations of the crystallites are influenced

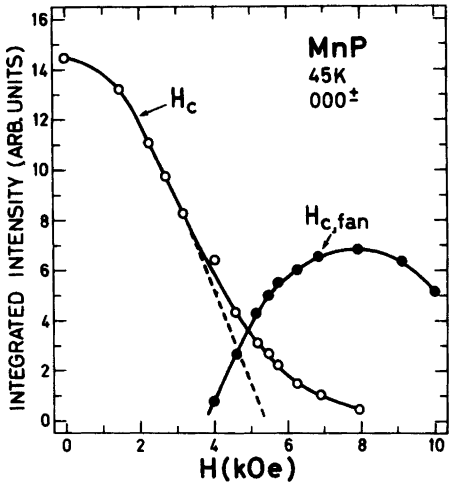

Fig. 8. Integrated intensities of $000^{\pm}$ for H_c and $H_{c,fan}$ *versus* applied field for MnP at 45 K.

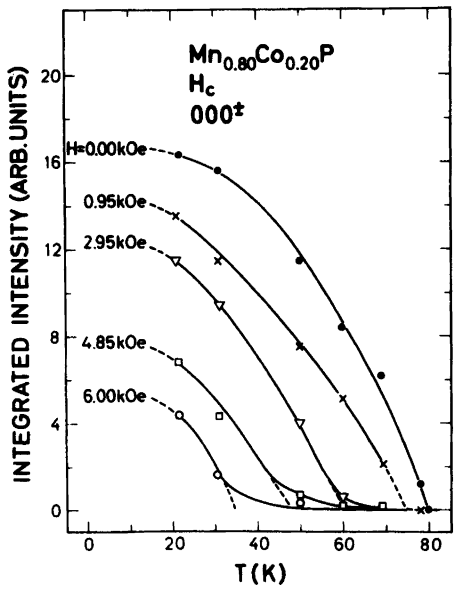

Fig. 9. Integrated intensity of $000^{\pm}$ for H_c (and possibly $H_{c,cone}$) of $Mn_{0.80}Co_{0.20}P$ *versus* temperature for various applied magnetic fields.

by the external field. Figs. 9 and 10 show that the $H_c/H_{c,cone}$ and $H_{c,fan}$ phases for an $Mn_{0.80}Co_{0.20}P$ powder sample coexist over considerable ranges

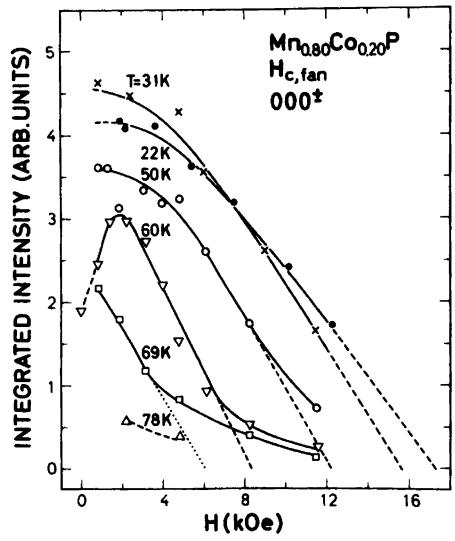

Fig. 10. Integrated intensity of $000^{\pm}$ for $H_{c,fan}$ of $Mn_{0.80}Co_{0.20}P$ *versus* applied magnetic field for various temperatures.

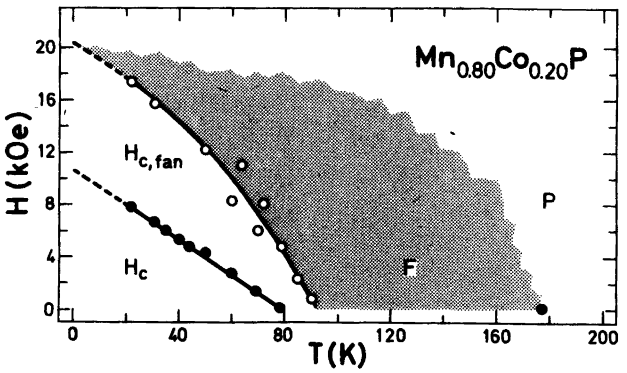

Fig. 11. "Partial powder H,T phase diagram" for $Mn_{0.80}Co_{0.20}P$. Abbreviations are defined in the caption to Fig. 7. See text.

of temperature and applied field. (Note that in order to illustrate both ways of representing the data, Fig. 9 shows curves for constant applied field, whereas Fig. 10 gives isotherms. The integrated intensity data are deduced from partially resolved peak profiles of the type exposed in Fig. 6.) The most interesting feature of these data is that the $H_{c,fan}$ state of the $Mn_{0.80}Co_{0.20}P$ powder sample can be induced by very low fields; at 60 K on application of approximately zero field. This appears to imply that the critical field for the H_c to $H_{c,fan}$ conversion (presumably for **H**||**a**, *vide supra*) is very small for $Mn_{0.80}Co_{0.20}P$. From the extrapolated temperatures and fields for the disappearance of the $H_c/H_{c,cone}$ and $H_{c,fan}$ phases in Figs. 9 and 10, the "partial powder H,T phase diagram" for $Mn_{0.80}Co_{0.20}P$ in Fig. 11 has been sketched. It should be emphasized that the points and curves shown on this diagram refer to the disappearance of the phases in question, and that most of the region marked H_c also includes $H_{c,fan}$ (and possibly $H_{c,cone}$) as additional phase(s). Similarly also ferromagnetic order is likely to be present for $H>0$ kOe. However, due to the relatively small amounts of the F phase present, and the difficulties involved in establishing a ferromagnetic contribution to the nuclear reflections, the coexistence of the $H_{c,fan}$ and F phases could not be ascertained. The possibility that the P, F, $H_{c,fan}$ triple point(s) in the H,T diagram(s) with **H**||**a** (and **H**||**c**) for $Mn_{0.80}Co_{0.20}P$ is (are) Lifshitz point(s) will be tested on single

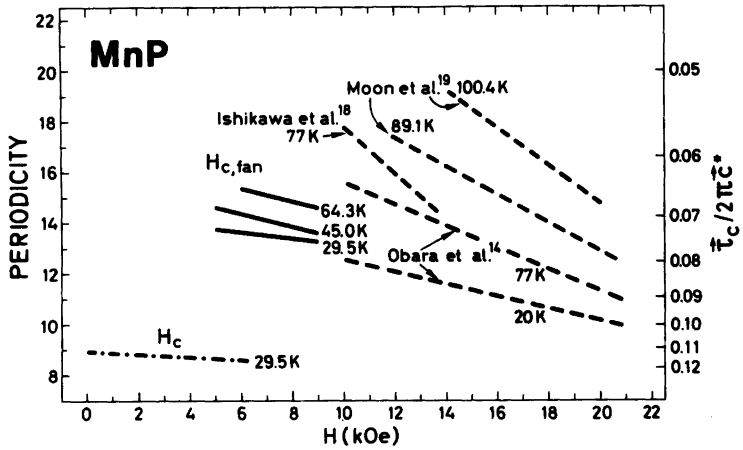

Fig. 12. Periodicities of H_c and $H_{c,fan}$ for MnP as function of applied magnetic field. References to earlier works are given on the illustration.

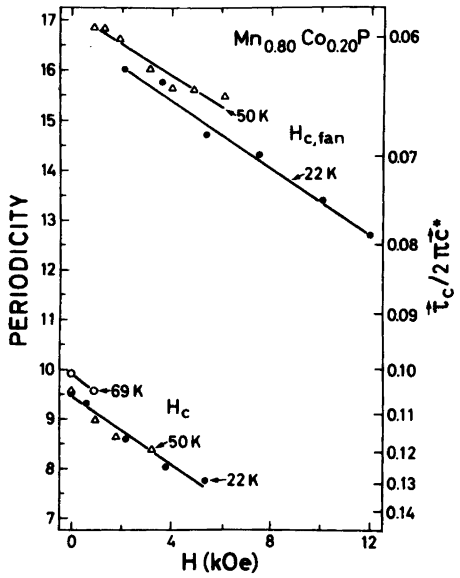

Fig. 13. Periodicities of H_c and $H_{c,fan}$ for $Mn_{0.80}Co_{0.20}P$ as function of applied magnetic field.

crystals which have been obtained during this study.

The propagation vector of a spiral structure is open for quite accurate determination even on powder samples. The τ_c *versus H* relationships for the H_c and $H_{c,fan}$ phases of MnP are shown in Fig. 12 for various temperatures, experimental points being omitted for clarity reasons. A scale which is linear in the periodicity (*viz.* the reciprocal propagation vector, $|\tau_c|^{-1}$) is used in the illustration. This gives linear $|\tau_c|^{-1}$ *versus H* curves. The present results for the $H_{c,fan}$ state are seen to comply with the findings in Refs. 14 and 19. The field dependence of the periodicity reported in Ref. 18 is a factor of two too large. Fig. 12 brings out a pronounced difference in the size as well as in the field dependence of the periodicity between the H_c and $H_{c,fan}$ phases. The present results for the H_c phase of MnP are essentially consistent with those of Obara *et al.*[14] who report that the periodicity is temperature and field independent. (Obara *et al.* give no numerical data in support of this statement. On this background the about 10 % change in τ_c or $|\tau_c|^{-1}$ with T (Fig. 3) and the about 5 % change in $|\tau_c|^{-1}$ with *H* (Fig. 12) may be acceptable.)

The variations in the periodicity of H_c and $H_{c,fan}$ for $Mn_{0.80}Co_{0.20}P$ with the applied field is shown in Fig. 13. The fairly large difference between the periodicities of H_c and $H_{c,fan}$ is seen to be maintained also for $Mn_{0.80}Co_{0.20}P$. A prominent difference between MnP and $Mn_{0.80}Co_{0.20}P$ is that $|\tau_c|^{-1}$ for H_c and $H_{c,fan}$ exhibits approximately equal field dependences for $Mn_{0.80}Co_{0.20}P$. The slope of the periodicity *versus* applied field lines is, at comparable temperatures, considerably larger for both H_c and $H_{c,fan}$ for $Mn_{0.80}Co_{0.20}P$ than for MnP.

Acknowledgements. This work has received financial support from The Norwegian Research Council for Science and the Humanities. The authors are also grateful to Dr. J. Als-Nielsen for the opportunity to perform the neutron diffraction experiments in external magnetic fields at Risø, Denmark.

REFERENCES

1. *Gmelins Handbook of Inorganic Chemistry, System No. 56: Manganese, Vol. C9,* Berlin–Heidelberg–New York 1983.
2. Fjellvåg, H., Kjekshus, A., Zięba, A. and Foner, S. *J. Phys. Chem. Solids 45* (1984). In press.
3. Selte, K., Birkeland, L. and Kjekshus, A. *Acta Chem. Scand. A 32* (1978) 731.
4. Fjellvåg, H. and Kjekshus, A. *Acta Chem. Scand. A 38* (1984) 1.
5. Fjellvåg, H. and Kjekshus, A. *To be published.*
6. Bacon, G. E. In Yelon, W. B., Ed., *Neutron Diffraction Newsletter,* Columbia 1977.
7. Watson, R. E. and Freeman, A. J. *Acta Crystallogr. 14* (1961) 27.
8. Selte, K. and Kjekshus, A. *Acta Chem. Scand. 27* (1973) 3195.
9. Endresen, K., Furuseth, S., Selte, K., Kjekshus, A., Rakke, T. and Andresen, A. F. *Acta Chem. Scand. A 31* (1977) 249.
10. Shapira, Y., Becerra, C. C., Oliveira, N. F. and Chang, T. S. *Phys. Rev. B 24* (1981) 2780.
11. Felcher, P. G. *J. Appl. Phys. 37* (1966) 1056.
12. Takase, A. and Kasuya, T. *J. Phys. Soc. Jpn. 49* (1980) 484.
13. Forsyth, J. B., Pickart, S. J. and Brown, P. J. *Proc. Phys. Soc. 88* (1966) 333.
14. Obara, H., Endoh, Y., Ishikawa, Y. and Komatsubara, T. *J. Phys. Soc. Jpn. 49* (1980) 928.

15. Iwata, N., Fujii, H. and Okamoto, T. *J. Phys. Soc. Jpn. 46* (1979) 778.
16. Moon, R. M. *J. Appl. Phys. 53* (1982) 1956.
17. Hiyamizu, S. and Nagamiya, T. *Int. J. Magn. 2* (1972) 33.
18. Ishikawa, Y., Komatsubara, T. and Hirahara, E. *Phys. Rev. Lett. 23* (1969) 532.
19. Moon, R. M., Cable, J. W. and Shapira, Y. *J. Appl. Phys. 52* (1981) 2025.
20. Komatsubara, T., Suzuki, T. and Hirahara, E. *J. Phys. Soc. Jpn. 28* (1970) 317.
21. Ishizaki, A., Komatsubara, T. and Hirahara, E. *Prog. Theor. Phys. Suppl. 46* (1970) 256.
22. Shapira, Y. and Oliveira, N. F. *Phys. Lett. A 89* (1982) 205.
23. Shapira, Y. In Pynn, R. and Skjeltorp, A. T., Eds., *Multicritical Phenomena,* Plenum, New York – London 1984.
24. Huber, E. E. and Ridgley, D. H. *Phys. Rev. A 44* (1964) 1033.

Received Februay 10, 1984.